Journal of Undergraduate Chemistry Research, **2024**, 23(3), 31

TRAP AND EXCIMER FLUORESCENCE INTENSIFICATION OF BIPHENYL AND NAPHTHALENE ON Al_2O_3 BY HEXANE, DICHLOROHEXANE AND *p*-XYLENE

Alan O. Lopez*, Jesse C. Nieman*, Jessica M. Rosenfeld*, Reese M. Toepfer* and A.M. Nishimura†

Department of Chemistry, Westmont College, Santa Barbara, CA 93108

Abstract

Vapor deposition of aromatic hydrocarbons formed adlayers that were amorphous initially and underwent disorder-to-order transition when the temperature of the substrate was ramped during the temperature programmed desorption (TPD) experiment. In bilayers where the overlayer is a fluorophore, such as biphenyl and naphthalene, the underlayer can be used to disrupt the morphology of the overlayer and this disruption can be observed by monitoring the fluorescence of the fluorophore during the TPD. 1,6-Dichlorohexane was found to enhance the fluorescence from traps for biphenyl and naphthalene, whereas hexane caused the formation of excimers. p-Xylene enhanced both the excimer and traps in these two adsorbates.

†Corresponding author: nishimu@westmont.edu *Undergraduate researchers and co-authors

Keywords: adsorption, naphthalene, biphenyl, excimer, vapor deposition, desorption, temperature programmed desorption, TPD

Submitted: July 10, 2024 Accepted: July 15, 2024 Published: July 29, 2024

Introduction

In a recent study, biphenyl was used to characterize the surface morphology that formed when 1-chloroalkanes were vapor deposited on an Al_2O_3 surface.[1] Due to dispersion forces, the alkyl chain organized to form adsorption sites if the length of the alkyl moiety was sufficient to accommodate the fluorophore.[2-5] This finding motivated an ancillary question: by careful choice of the underlayer, can the fluorophore be made to form a specific type of fluorescence emitter, namely trap or excimer, as the underlayer percolates through the fluorophore on its way to desorption?[1] 1,6-Dichlorohexane was an example of an underlayer that promoted the formation of traps after the disorder-to-order transition of biphenyl.[1] On the other hand, hexane was an example of a underlayer that promoted the growth of excimers.[1,6] *p*-Xylene served to enhance *both* the excimer and trap fluorescence.[11] Naphthalene was chosen as the other overlayer because, in contrast to biphenyl, its excimer fluorescence dominates the spectrum, with the appearence of a very weak trap intensity at the disorder-to-order transition just before desorption.[7-10] Hence any effect on excimer or trap fluorescence should be manifested by changes in these sources of emission. Details of these results are given in this paper.

Experimental

Biphenyl, naphthalene, 1,6-dichlorohexane, hexane and *p*-xylene of the highest purity (> 99%) were purchased from commercial sources (Sigma-Aldrich, St. Louis, MO). They were placed in a sample holder attached to one end of a precision leak valve for vapor deposition. The ultra-high vacuum chamber had a background hydrogen base pressure of 1 x 10^{-9} Torr. A single crystal of Al_2O_3 (0001) (Crystal Systems, Inc., Salem, MA) was suspended on the lower end of a liquid nitrogen cryostat via copper post on either side of the Al_2O_3 with a sapphire spacer for electrical and thermal isolation. Resistive heating of the Al_2O_3 was done by sending current through a thin tantalum foil that was in thermal contact with the substrate. A type-K (chromel/alumel) thermocouple (Omega, Norwalk, CT) that was also in thermal contact with the Al_2O_3 monitored the temperature. Process control during the TPD experiment was accomplished by a program written in LabVIEW (National Instruments, Austin, TX) that incorporated a PID (proportional-integral-derivative) feedback algorithm that linearly incremented the temperature of the Al_2O_3 crystal.

During the TPD, the LabVIEW program also took the fluorescence spectra every 300 ms in real time from an Ocean Optics USB4000 spectrometer (Ocean Optics, Dunedin, FL) that was sensitive in the ultra-violet. Manipulation of the array of spectra as a function of temperature by a MATLAB (Mathworks, Natick, MA) template yielded the WRTPD (wavelength resolved TPD) that are shown in the figures. To ensure a clean surface, the Al_2O_3 was heated to 300 K after each run. Temperature ramps to higher temperatures did not indicate any other adsorbates.[7-10]

The activation energy for desorption, E_a, was calculated by Redhead analysis in which a first-order desorption kinetics as described by King was assumed and is based on the mass spectral peak desorption temperature, T_p.[12-14] The uncertainties in the desorption temperatures lead to a propagated error in the activation energies of ± 2%.

The LabVIEW program received data from a residual gas analyzer so that both the deposition and the desorption of biphenyl could be monitored. The surface coverages, Θ, in monolayers (ML) were calculated by calibrating the integrated mass spectral peaks to an optical interference experiment. The interference experiment yielded accurate rate of deposition with coverage error of ± 30%, and is described in detail elsewhere .[7-10]

For surface coverages in the multilayer regime, multidimensional nucleation and crystal growth are expected at the disorder-to-order transition. In order to model the disorder-to-order transition as a nucleation-crystallization process, the Avrami model was used.[15] The Avrami equation is given by:

$$I(t) = e^{-kt^n}$$

where **I**(t) is the time dependent fluorescence intensity at the disorder-to-order transition that is converted to fraction of the disordered state at the transition, **k** is related to the rate with which crystallization occurs and is in part, a function of the density of nucleation sites, **t** is time in s and **n** is the dimensionless Avrami exponent that yields the dimensionality of the nucleation-crystallization process.[15] The unit for **k** is the inverse of time raised to the n^{th} power. This expression was made to fit the wavelength-resolved TPD data at the disorder-to-order transition using

algorithms provided by SciPy (an open-source Python library) and automated with Python (an open-source programming language, Python Software Foundation) in which the parameters were controlled by user interface.

In order to more accurately report the relative spectral intensities of overlapping peaks, spectral deconvolution was accomplished and reported as plots of the intensities as function of adlayer coverages. Codes were written around Igor pro 8.04. (WaveMetrics, Lake Oswego, OR) so that linear combinations of lineshape (gaussian or lorentzian) were deconvoluted from the wavelength-resolved TPD data. The output of the program yielded the peak height, the standard deviation (full-width-at-half of the maximum intensity, FWHM), and the wavelength at the center of the peak.

In order to find a correlation between the biphenyl's dihedral angle and its fluorescence λ_{max}, a study of 11 biphenyl molecular species with 2,2'dimethylbiphenyl on one extreme with a dihedral angle of 90º and 9,10-dihydrophenanthrene with a dihedral angle of 0º were plotted.[17] The trendline equation was a second-order polynomial which was then used to generate a dihedral angle to biphenyl compound from the λ_{max} of biphenyl compound in any molecular environment.[17] The error in the dihedral angle has been estimated to be around ± 10%.[17]

Results and Discussion

Vapor deposition resulted in an amorphous arrangement of adsorbate molecules in the adlayer.[1,6-11] During the TPD, adlayers transitioned from the intial amorphous morphology to a more ordered state.[1,6] In a bilayer, if the underlayer has a lower desorption temperature than the overlayer, the underlayer molecules will percolate through the overlayer before desorbing during the TPD procedure.[1,6] The interaction with the underlayer molecules during percolation typically will have an effect on the morphology of the fluorophore. By judicious choice of the underlayer, the morphology of the overlayer can be manipulated in such a way that ordering in the orderlayer can be forced to occur by the underlayer providing nucleation sites or if the overlayer is ordered when the underlayer comes through, the order in the overlayer can be fractured, thereby increasing the density of defect sites from which radiative relaxation can occur. The result is enhanced monomeric fluorescence. If the underlayer during its passage, causes additional disorder in the overlayer, enhanced fluorescence intensity that is excimeric may result.

1,6-Dichlorohexane: Underlayer Molecule that Caused Disorder in the Ordered Biphenyl and Naphthalene Fluorophores

1,6-Dichlorohexane/Biphenyl

In previous studies, fluorophores were used to probe the morphological changes that occur during a TPD procedure on vapor deposited biphenyl adlayers on Al_2O_3.[1,6] The peak desorption temperature, T_p, of neat biphenyl at low coverages was 229 K. First-order desorption was assumed and the activation energy for desorption, E_a, was calculated to be 59.5 kJ/mol.[11-13] Upon deposition, excitation of neat biphenyl on the Al_2O_3 surface with a high-pressure Hg lamp caused the amorphous biphenyl to fluoresce with a λ_{max} at 318 nm. As described in the experimental section, the dihedral angle of the biphenyl at this wavelength was calculated to be 41 ± 4º.[16] As can be seen from Figure 1, when the surface temperature was linearly ramped in a TPD experiment, the biphenyl adlayer underwent a disorder-to-order transition at 160 K, where λ_{max} red-shifted to 340 nm and the overall intensity decreased. The dihedral angle at this wavelength was 4º.[16] Since energy hopping in an ordered matrix is nonradiative, the reduction in intensity arose partly from the ordered planar biphenyl that became energy carriers for the trap sites from which fluorescence occurred.[15]

When 1,6-dichlorohexane was deposited as an underlayer, the biphenyl trap intensity was observed to dramatically increase and peaked at 218 K subsequent to the desorption of the underlayer at 212 K. This is shown in Figure 2. In order to determine if there exists an optimum annealing temperature for the 1,6-dichlorohexane that

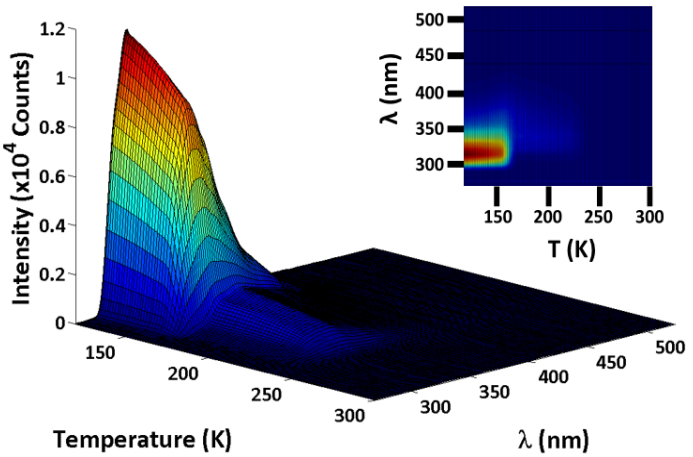

Figure 1: Wavelength-resolved TPD of biphenyl with a λ_{max} at 318 nm. The disorder-to-order transition occurred at about 160 K and λ_{max} shifted to 340 nm. $\Theta_{biphenyl}$ ~ 97 ML. Inset: Top view.

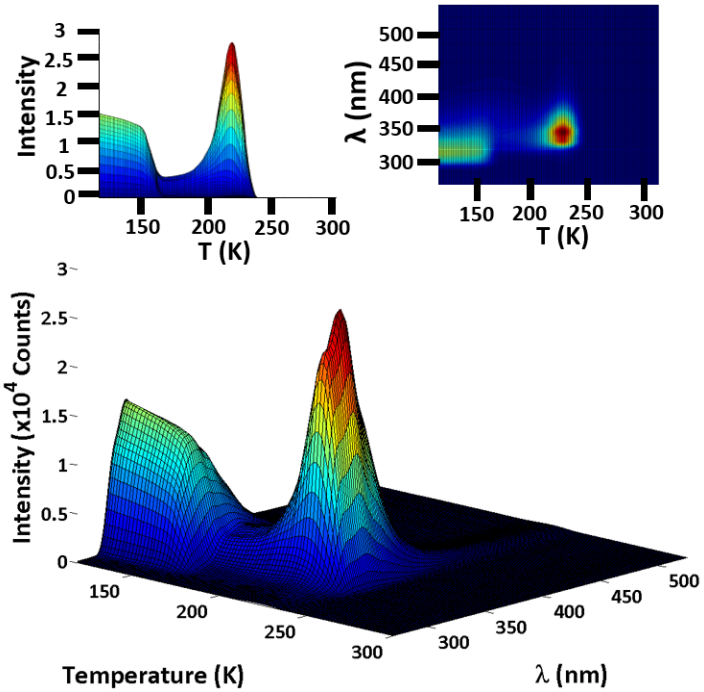

Figure 2. Wavelength-resolved TPD of a bilayer of 1,6-dichlorohexane and biphenyl with $\Theta_{1,6\text{-dichlorohexane}}$ ~ 108 ML with a overlayer of $\Theta_{biphenyl}$ ~ 102 ML During the TPD, the twisted conformer with λ_{max} of 318 nm dominate at deposition, and at up to 160 K. This conformer underwent disorder-to-order transition and the trap fluorescence at 218 K appears as a doublet with λ_{max} of 330 nm and 345 nm the intensity of which was dependent on the $\Theta_{1,6\text{-dichlorohexane}}$ coverage. Left and right insets: side and top views, respectively.

yielded the largest fluorescence intensity from the trap at 218 K, the intensities of the doublet at 330 and 345 nm peaks as a function of the annealing temperature were plotted and are shown in Figure 3. Tentatively this doublet has been assigned to a C-C stretching vibration. The 0,0 transitional wavelength of 330 nm correspond to dihedral angle of 18º for the conformer of biphenyl from which the fluorescence originated.[16] Since annealing at 130 K enhanced the trap intensity sufficiently, this annealing temperature was used in all subsequent experiments. Since 1,6-dichlorohexane desorbs at 212 K, which is 17 K lower than the desorption temeprature of biphenyl, the underlayer intruded through the biphenyl overlayer that left a wake of defect sites from which radiative relaxation occurred that resulted in the increased intensity.

In Figure 4, the deconvoluted peak areas of the 330 and 345 nm lines were plotted as a function of the 1,6-dichlorohexane coverages, while biphenyl coverage was held constant at 99

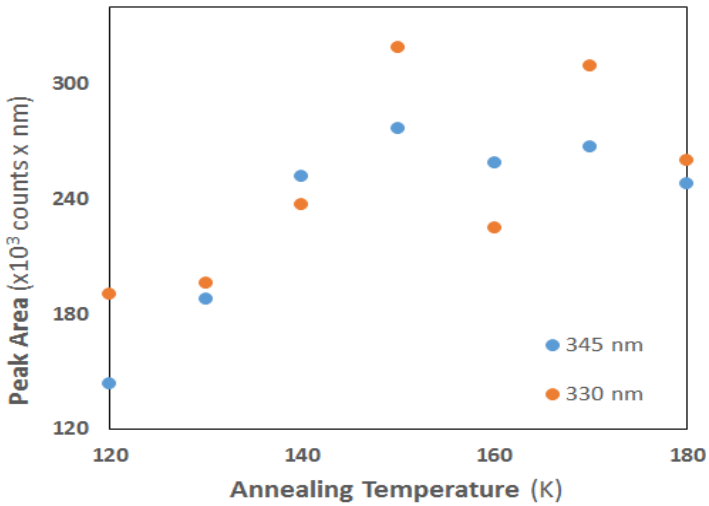

Figure 3. To determine the optimum annealing temperature, both $\Theta_{1,6\text{-dichlorohexane}}$ and $\Theta_{biphenyl}$ were kept constant at 113 ± 13 ML and 96 ± 6 ML, respectively, while the annealing temperature was varied. The intensities at λ_{max} = 330 and 345 nm were monitored at 218 K during the TPD. The plot shows the deconvoluted peak areas as a function of annealing temperature in K.

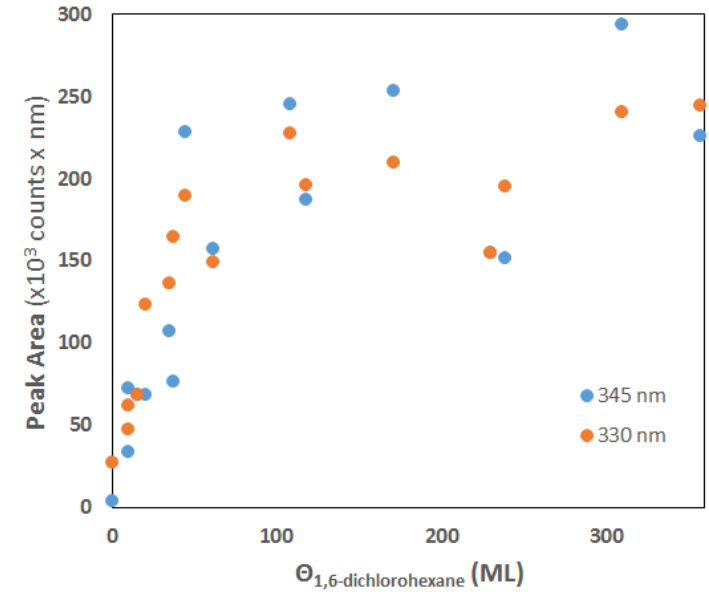

Figure 4. Integrals of the deconvoluted fluorescence peaks of biphenyl at 330 and 345 nm as a function of the annealed 1,6-dichlorohexane, $\Theta_{1,6\text{-dichlorohexane}}$ while the biphenyl coverage was held constant at $\Theta_{biphenyl}$ ~ 99 ± 11 ML. The integrals were measured at 219 ± 2 K.

ML. It appears that there is a leveling of the slope at about 100 ML of 1,6-dichlorohexane. Hence the passage of additional 1,6-dichlorohexane did not further break down the order in the biphenyl overlayer.

1,6-dichlorohexane/naphthalene

The adlayer that forms when naphthalene is vapor deposited on Al_2O_3 is amorphous. Optical pumping of the singlet electronic state gave rise to excimer fluorescence that has been so categorized because of the observed broad and featureless spectrum.[17] As the temperature of the Al_2O_3 substrate was raised in a TPD experiment, naphthalene underwent a disorder-to-order transition at about 180 K, at which temperature the spectrum changed to that observed for the monomer with two peaks at 325 and 334 nm. The doublet was due to the strong vibrational progression that has been attributed to a C-H bending vibration.[8-11]

An underlayer that has a lower T_p can cause naphthalene to undergo its disorder-to-order transition at a lower than normal temperature by providing the nucleation sites for crystallization. If on the other hand, the T_p of the underlayer is *higher* than the disorder-to-order transition in naphthalene, its disorption can enhance the formation of excimers.

Shown in Figure 5 is the wavelength resolved TPD of 93 ML multilayer naphthalene. Figure 6 shows the wavelength resolved TPD of naphthalene with 18 ML of 1,6-dichlorohexane and 97 ML of naphthalene. What was immediately apparent was that the trap emission was enhanced by the desorption of 1,6-dichlorohexane at 201 K during the TPD. Additionally, the initial excimer intensity with the underlayer is higher by almost 2x with just 18 ML of 1,6-dichlorohexane.

To understand why 1,6-dichlorohexane served to increase the trap emission in naphthalene, 1,6-dichlorohexane was kept constant at 30 ± 6 ML, while the coverage of naphthalene was varied. The results are shown in Figure 7. The deconvoluted peak areas of the excimer at 400 nm and the trap emission from naphthalene

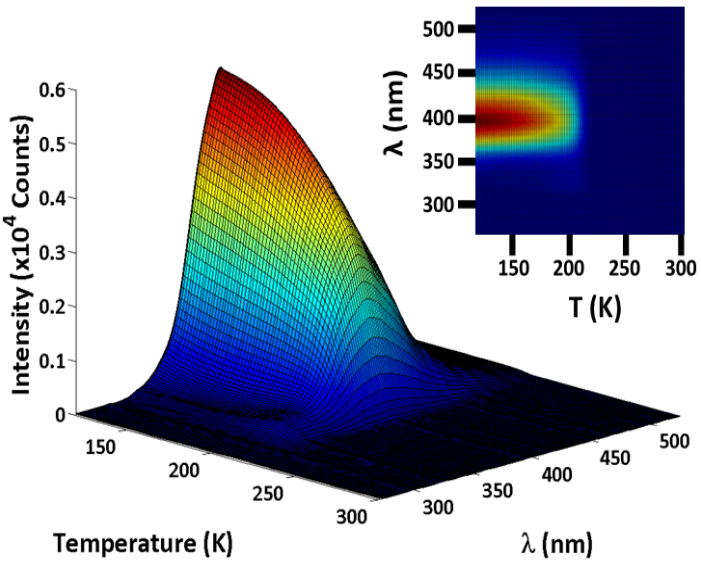

Figure 5. Wavelength-resolved TPD of naphthalene with $\Theta_{naphthalene}$ ~ 93 ML that had been deposited at 117 K. The λ_{max} of 400 nm excimer dominate the spectrum. The disorder-to-order transition that occurred at 200 K with a blue-shifted doublet with λ_{max} of 325 and 334 nm that is barely visible. Inset: top view.

monomers at 347 nm were plotted as a function of the naphthalene coverage. It is apparent that the intensity of the excimer and the trap increases monotonically with coverage.

Figure 8 shows the effect of 1,6-dichlorohexane as it gains thermal energy and as it begins to percolate through the naphthalene adlayer, the trap emission is enhanced. The integrals of the deconvoluted 347 nm peak were plotted as a function of 1,6-dichlorohexane coverages. Here, the coverage of naphthalene was held constant at 100 ML. As can be seen from Figure 8, the trap peak hight can reach up to almost one half that of the excimer peak height even at very low 1,6-dichlorohexane coverages, but the slope levels at about 50 ML in Figure 6, left inset. This leveling of the slope is difficult to explain. Perhaps the intrusion causes sufficent disorder to convert the ordered molecules to revert to excimer. More study that focuses on this issue is necessary. Although this effect was not consistently observed for all systems that were studied here, this was repeated in sufficient frequency to warrant further study.

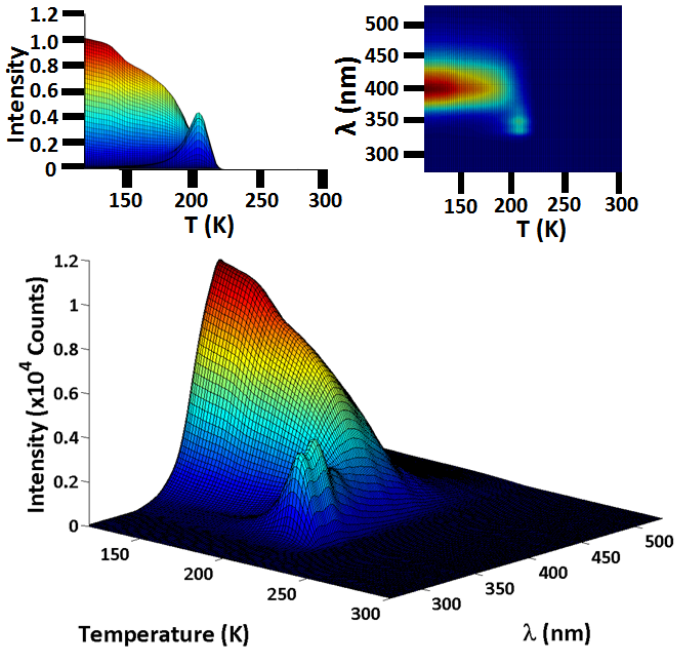

Figure 6. Wavelength-resolved TPD of naphthalene with $\Theta_{naphthalene}$ ~ 97 ML and an underlayer of 1,6-dichlorohexane with $\Theta_{1,6\text{-dichlorohexane}}$ ~ 18 ML. Maximum in the trap intensity at 201 K. Left and right insets: side view and top views, respectively.

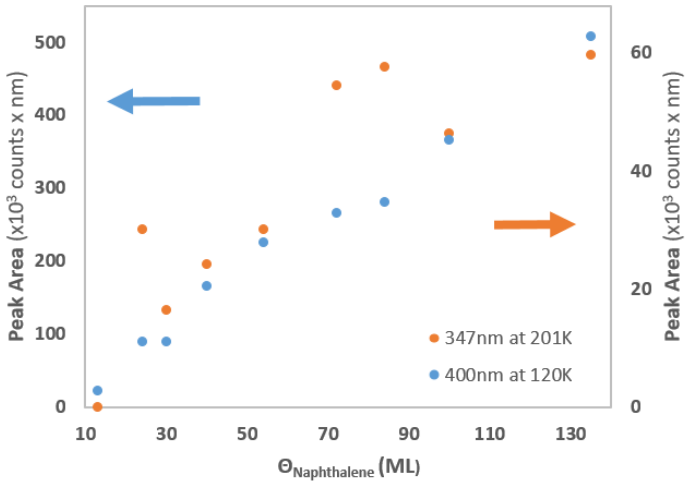

Figure 7. A plot of the integrals of the deconvoluted intensities of the excimer fluorescence of naphthalene at 395 nm (blue) at deposition and the trap intensities at 347 nm at 201 K (red) as a function of naphthalene coverage (ML). Coverage of 1,6-dichlorohexane was held constant at 30 ± 6 ML. The arrows point to the respective vertical scales.

Although the nucleation-crystallization kinetics have been analyzed for biphenyl,[6] they have not been done for naphthalene and for the 1,6-dichlorohexane/biphenyl bilayer. In Figure 9, the Avrami n- and k-values are plotted for the 1,6-dichlorohexane/naphthalene bilayer as a function of coverages of 1,6-dichlorohexane. The dimensionality and rate of propagation given by the n- and k-values, respectively, do not change from those that were determined for multilayer naphthalene. The assumption can be made that the percolation of 1,6-dichlorohexane through the naphthalene has little effect on the nucleation and propagation during the disorder-to-order transition in naphthalene. Note, however, that at about 30 ML of 1,6-dichlorohexane, the n-values dropped to almost 2 while the k-values increased. This discontinuity occurred at about the same coverage of 1,6-dichlorohexane, as the previous plot of the intensity of the trap fluorescence.

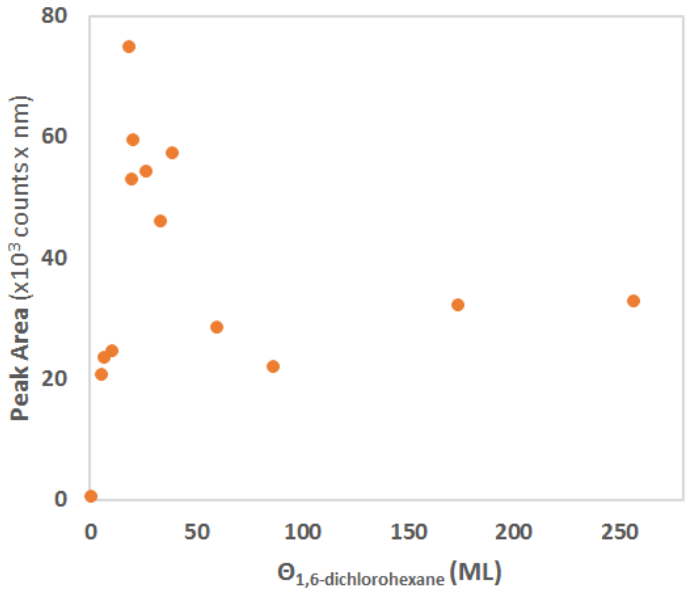

Figure 8. Plot of the integrals of the deconvoluted peak of the naphthalene trap at 347 nm as a function of $\Theta_{1,6\text{-dichlorohexane}}$ at 201 K during the TPD. Naphthalene coverage was held constant at 97 ± 19 ML.

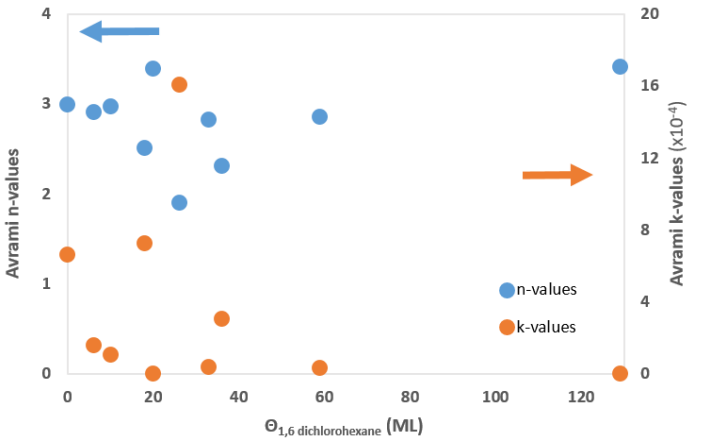

Figure 9. Plot of the Avrami n and k values for naphthalene as a function of the coverages of 1,6-dichlorohexane. The naphthalene coverage was fixed at 94 ± 35 –ML.

n-Hexane: Underlayer Molecule that Caused Additional Disorder in the Amorphous Biphenyl and Naphthalene Fluorophores

n-hexane/biphenyl

Shown in Figure 10 is the wavelength-resolved TPD of biphenyl with *n*-hexane as the underlayer. Low coverage *n*-hexane on Al_2O_3 has a T_p of 146 K and a E_a of 36 kJ/mol.[6] In contrast to Figure 1, the 318 nm fluorescence that is normally expected with the twisted conformer that dominate the fluorescence has almost disapeared, but the intensity is in the peaks at λ_{max} of 370 and 340 nm that has been assigned to the excimer and trap emissions, respectively. The trap emission orginated from biphenyl with a dihedral angle of 4º.[16] Then at 157 K, subsequent to the desorption of the *n*-hexane, these two peaks at 370 and 340 intensified to twice the initial intensities. (Cf. left inset in Figure 10) The percolation of *n*-hexane through the biphenyl caused those molecules that were in the twisted conformer to become planar. Hence as can be seen from the right inset, the emitting species are the excimer at 370 nm and the monomer at 340 nm. Then the disorder-to-order transition caused the excimeric species to become monomeric and ordered. Consequently, the fluorescence wavelength shifted to 340 nm and this planar conformer of biphenyl was the only emitter past the disorder-to-order transition during the TPD.

In Figure 11 is shown the integrals of deconvoluted intensities of the excimer at 370 nm (blue) and the monomeric trap intensities at 340 nm (orange) plotted as a function of *n*-hexane coverages. Two features can be noted: first, deconvolution of the peaks at 156 K during the TPD (Cf. right inset in Figure 10), resulted in the intensity mostly arising from the excimer at 370 nm, even though a cursory look might indicate that the two peaks are of similar intensities. Second, the enhancement of the excimer intensity was as much as 2 times higher than the initial intensity even at low coverages, of about 50 ML of *n*-hexane.(Cf. Figure 10, left inset). This was a good indicator of the degree to which the twisted conformer was made planar by *n*-hexane. The appearance of excimer clearly indicateed that the adlayer was amorphous, as that was the morphology of adlayer that was required for the surface formation of excimers.[1,6,16]

n-hexane/naphthalene

Shown in Figure 12 is the wavelength-resolved TPD of naphthalene with *n*-hexane as the underlayer. Comparison with Figure 5 shows that the excimer intensity increased dramatically. This

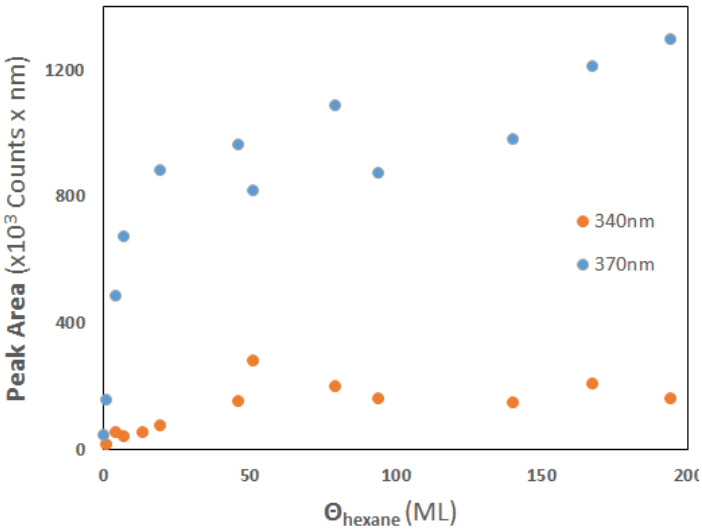

Figure 11: For *n*-hexane/biphenyl bilayer, plot of the integrals of the deconvoluted trap at λ_{max} of 340 nm (orange) and excimer at 370 nm (blue) as a function of *n*-hexane coverage at 157 ±2 K during the TPD. Biphenyl coverage was held constant at 97 ML.

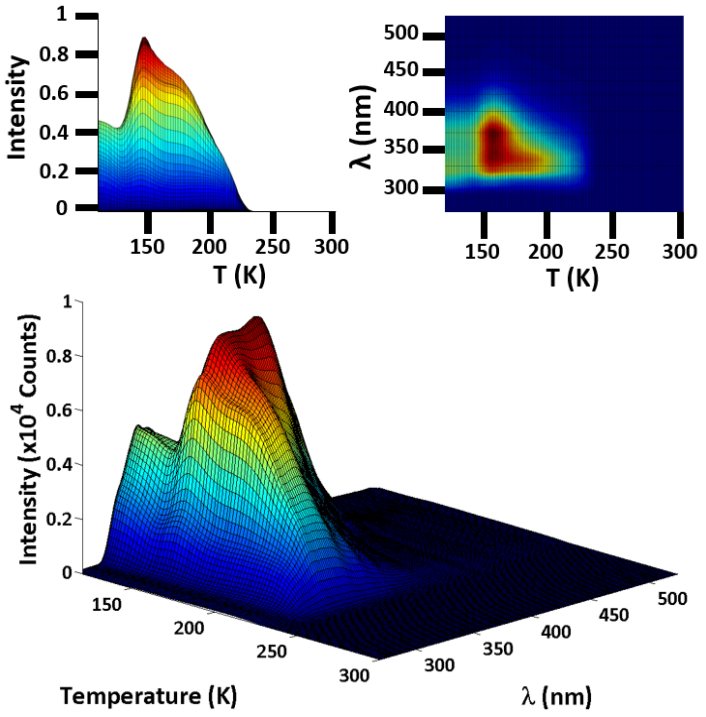

Figure 10: Wavelength-resolved TPD of biphenyl with $\Theta_{n\text{-hexane}}$ = 87 ML and $\Theta_{biphenyl}$ 107 ML. The λ_{max} at 320 nm peak that is usually observed at deposition has minimal intensity. At 156 ±1.4 K, the fluorescence intensities at λ_{max} 340 nm and 370 nm are enhanced. Left and right insets: side view and top views, respectively.

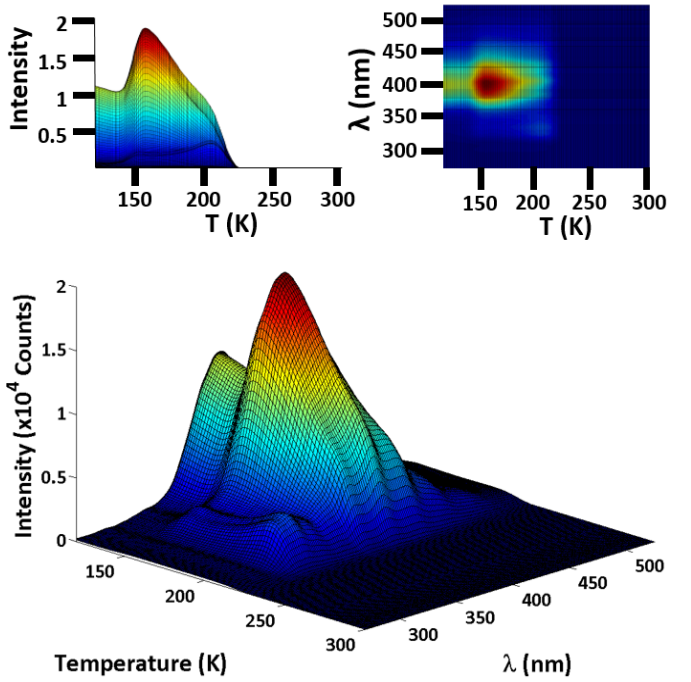

Figure 12: Wavelength resolved TPD of *n*-hexane/naphthalene bilayer with $\Theta_{n\text{-hexane}}$ = 48 ML and $\Theta_{naphthalene}$ = 101 ML. The excimer with λ_{max} of 395 nm dominates the spectrum. The enhanced excimer fluorescence appears at 157 ± 2 K with the growth of traps that increases until a maximum at 204 K. Left and right insets: side and top views, respectively.

increase was observed at 157 ± 2 K, and was the same as with biphenyl as the overlayer. Note that at this temperature, the disorder-to-order transition commenced and continued with normal increase in intensity that reached a maximum at about 204 K, followed by desorption.

Shown in Figure 13 is the plot of the relative intensities of the excimer at 370 nm at 204 K during TPD to that of the excimer at deposition. Although the enhancement is monotonically increasing, the slope decreased at *n*-hexane coverages greater than 100 ML. This makes sense because of the finite thickness of the perturbing *n*-hexane layer that moved through the naphthalene adlayer and in doing so, the extent to which a ML of *n*-hexane molecules affected the naphthalene molecules remained the same.

*p-Xylene: Underlayer Molecule that Caused Disorder in the Ordered **and** Amorphous Biphenyl and Naphthalene Fluorophores*

p-xylene/biphenyl

p-Xylene desorbs at 180 K, and its activation energy of desorption was 47 kJ/mol. These are summarized in Table 1. When the *p*-xylene was deposited and annealed to 160 K as an underlayer to biphenyl, the excimer fluorescence dominated the spectrum as seen in Figure 14. Subsequent to the disorder-to-order transition during the TPD, peaks appeared at 320, 335, 350, and 370 nm that increased to a maximum at 192 ± 10 K. All of these peaks behaved similarly with *p*-xylene coverage. Therefore, the 350 nm peak was chosen as a representative and is plotted as a function of *p*-xylene coverage with a fixed biphenyl coverage at 66 ±6 ML in Figure 15. There appears to be a leveling of the slope at about 100 ML of *p*-xylene.

p-xylene/naphthalene

Shown in Figure 16 is the wavelength-resolved TPD of bilayer of *p*-xylene and naphthene, in which *p*-xylene was annealed at 160 K prior to the deposition of naphthalene. Shown in Figure 17 are the plots of areas of selected deconvoluted fluorescence peaks as a function of *p*-xylene coverages. The naphthalene coverage was held constant at 100 ± 14 ML. At 188 ± 3K, the maxima in both the excimer and trap emissions were observed. The first trap peak at 320 nm has the largest area of the trap peaks and is plotted in blue. The peak at 400 nm is associated with excimer and appears to be the most intense and is in orange. Although not shown here, the 425 nm peak actually has the largest area when deconvoluted. The deconvoluted areas for the 320 and 400 nm peaks have been normalized against the intensity of the 400 nm excimer peak at deposition. It should be noticed that this initial peak has a large area (Cf. Figure 16) and that is the reason why the ratios are rel-

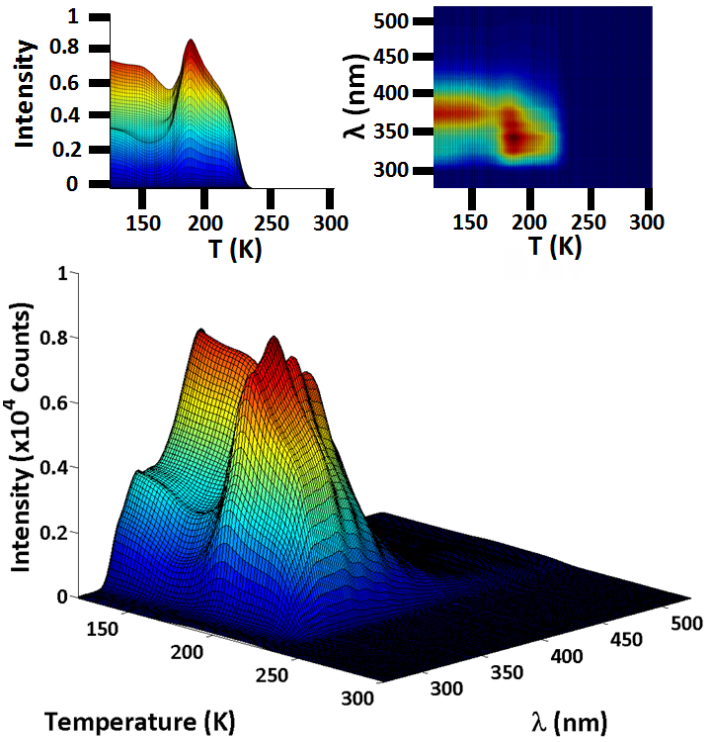

Figure 14: Wavelength resolved TPD of *p*-xylene/biphenyl bilayer with $\Theta_{p\text{-xylene}}$ = 24 ML and $\Theta_{biphenyl}$ = 58 ML. The excimer with λ_{max} of 400 nm dominates the spectrum. The enhanced excimer fluorescence appears at 192 ± 10 K. Left and right insets: side and top views, respectively.

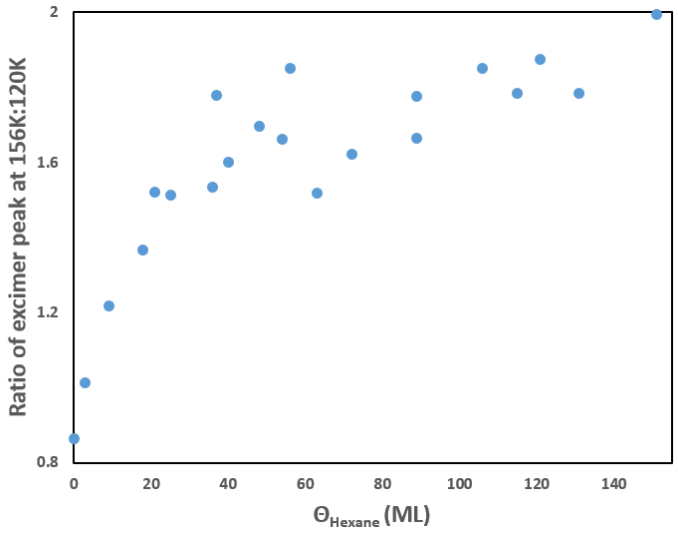

Figure 13: For *n*-hexane/naphthalene bilayer, plot of the ratio of the excimer intensity due to naphthalene at 160 K to the eximer intensity at the depositition temperature as a function of hexane coverage with λ_{max} at 400 nm at 157 ±2 K during the TPD subsequent to the desorption of *n*-hexane. The naphthalene coverage was held constant at $\Theta_{naphthalene}$ = 97 ± 12 ML

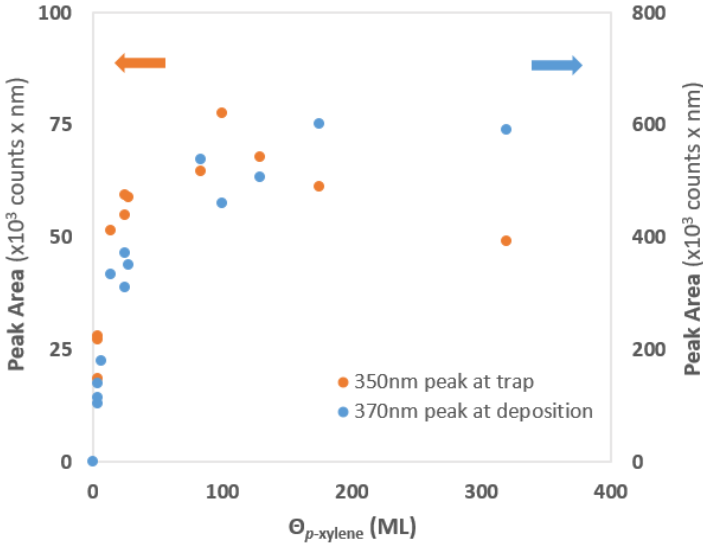

Figure 15: Plots of areas of selected deconvoluted fluorescence peaks for *p*-xylene/biphenyl bilayer with $\Theta_{biphenyl}$ = 66 ±6 ML. The excimer with λ_{max} of 370 nm dominates the spectrum at the start of the TPD. The trap intensity was measured at 192±10 K. Left and right insets: side and top views, respectively.

atively small. As was observed previously in 1,6-dichlorohexane/napthalene bilayer, there is a maximum in the areas of the deconvoluted peaks that appears at just less than 200 ML.

Summary

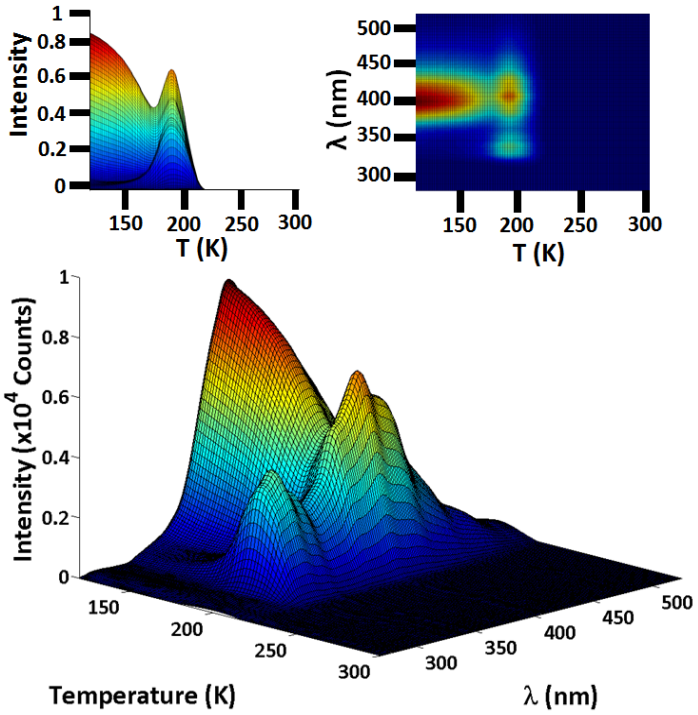

Figure 16: Wavelength resolved TPD of *p*-xylene/naphthalene bilayer with $\Theta_{p\text{-xylenexane}}$ = 104 ML and $\Theta_{naphthalene}$ = 102 ML. The excimer with λ_{max} of 400 nm dominatese spectrum. The enhanced excimer fluorescence appears at 188 ±3 K with the growth of traps that increases until a maximum at the same temperature. Left and right insets: side and top views, respectively.

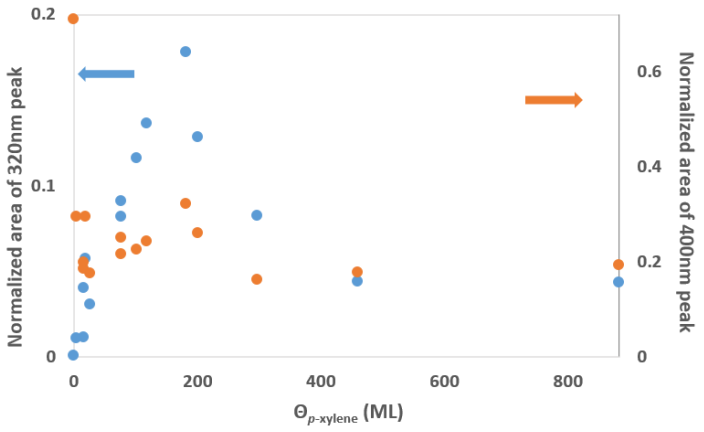

Figure 17: Plot of the ratio of the integrated areas of the deconvoluted peaks of naphthalene as a function of *p*-xylene coverages. The two peaks at 320 nm (trap) and 400 nm (excimer) were normalized against the excimer at deposition. Hence, 320 nm trap at 188 K/excimer at deposition in blue and 400 nm excimer peak at 188 K/excimer at deposition in orange.

Table 1: Summary of relevant data for the molecular systems reported here. Shown are adsorbates in the study, their T_p (K), E_a (kJ/mol), temperature at which the maximum intensities were observed (K), the peak wavelengths (nm) of species that were formed as a result of the underlayer molecules.

adsorbate	T_P (K)	E_a (kJ/mol)	overlayer	T @ I_{max} (K)	λ_{max}(nm)	overlayer	T @ I_{max} (K)	λ_{max}(nm)
1,6-dichlorohexane	212 ± 3	55 ± 1	biphenyl	218 ± 4	330†,345*†	naphthalene	201 ± 6	332,347*†
n-hexane	146 ± 2	36 ± 1	biphenyl	156 ± 1	320,340†,370*†	naphthalene	157 ± 2	400*†
p-xylene	180 ± 5	46.5 ± 1.5	biphenyl	192 ± 10	320,335,350*†,370	naphthalene	188 ± 3	320†,400†,425*
biphenyl	229 ± 1	59.5 ± 0.5						
naphthalene	215 ± 1	55 ± 0.5						

*most intense †plotted

In summary, the difference in the mechanism by which 1,6-dichlorohexane, hexane and *p*-xylene affect the overlayer can be gathered by the desorption temperatures in the bilayer. When *n*-hexane with T_p of 146 K was the underlayer, the desorption tempertures were consistently the same 157 ± 3 K for both of the overlayers, biphenyl and naphthalene. Here, *n*-hexane bolsters the adsorbate to maintain the disorder and to create sites upon which the planar form of the adsorbate fits into its structure. Thereby the planar form of biphenyl and the density of naphthalene excimer is increased. In other words, *n*-hexane serves as a intermediate adsorbent upon which the overlayer can adsorb.

On the other hand, the temperatures at which 1,6-dichlorohexane with a T_p of 212 ± 4 K yielded maximum in the excimer intensities varied: 218 ± 4 K for biphenyl and 201 ± 6 K for naphthalene. In these case, the 1,6-dichlorohexane had the effect of fracturing the ordered structure with biphenyl, since the disorder-to-order transitions for biphenyl had occurred at a lower temperature, appoximately 160 K. For naphthalene, 1,6-dichlorohexane created sufficient nucleation sites so that the excimer was encouraged to crystallize out.

Hence the hexane can be modeled to percolate through the biphenyl and naphthalene overlayers without much difficulty, but for 1,6-dichlorohexane, the comparatively larger size and electronegativity of the intruding molecule perturbed the overall morphology of the fluorophoric adlayer. When *p*-xylene was the underlayer to both biphenyl and naphthalene, it served to do both, that is, its disturbance served to assemble the biphenyl and naphthalene to form excimer, and formed nucleation sites for crystallization to occur.

Acknowledgment

The authors would like to thank the John Stauffer Charitable Trust for funding the student stipends for summer research.

References

1. J.M. Rosenfeld, R.M. Toepfer, A.O. Lopez, J.C. Nieman, I. Felix, J. Zerwas and A.M. Nishimura, *JUCR*, **2024.** 23, **2024**.
2. M. Frederick, J. Fowkes, *J. Phys. Chem*., **1980**, 84, 510-512.
3. M. Anwar, F. Turci and T. Schilling, *J. Chem. Phys.* **2013**, 139, 214904.
4. T. Arnold, C.C. Dong, R.K. Thomas, M.A. Castro, A. Perdigon, S.M. Clarke and A. Inaba, *Phys. Chem. Chem. Phys*.,**2002**, 4, 3430-3435.
5. T. Arnold, R.K. Thomas, M.A. Castro, S.M. Clarke, L. Messe and A. Inaba, *Phys. Chem. Chem. Phys*., **2002**, 4, 345-351.
6. I.Z. Song, S.T. Watanabe and A.M. Nishimura, *JUCR*, **2023**, 22, 78-85.
7. M.K. Condie, C. Kim, Z.E. Moreau, B. Dionisio, K. Nili, J. Francis, C. Tran, S. Nakaoka and A.M. Nishimura, *JUCR*, **2020**, 19, 14-17.
8. M.K. Condie, Z.E. Moreau and A.M. Nishimura *JUCR*, **2019**, 18, 15-18.
9. M.K. Condie, B.D. Fonda, Z.E. Moreau and A.M. Nishimura, *Thin Solid Films*, **2020**, 697, 137823-137828.
10. B.D. Fonda, Z.I. Shih, J.J. Wong, L.G. Foltz, K.A. Martin and A.M. Nishimura, *JUCR*, **2018**, 17, 32-35.
11. K.L. Nili, Z.E. Moreau and A.M. Nishimura, *JUCR*, **2020**, 19,

19-23.
12. P.A. Redhead. *Vacuum*, **1962**, 12, 203-211.
13. F.M. Lord and J.S. Kittelberger. *Surf. Sci.*, **1974**, 43, 173-182.
14. D.A. King. *Surf. Sci*., **1975**, 47, 384-402.
15. M. Avrami, J. Chem. Phys. 1939, 7, 1103-1112; 1940, 8, 212-224.
16. J.B. Birks. Photophysics of Aromatic Molecules, John Wiley & Sons Ltd., New York, NY (1970), pp. 301-370.
17. N.M Bond and A.M. Nishimura *JUCR*, **2022**, 21, 84-92.